Simulation of XY model in a quantum computer

Author: Marc Farreras Bartra.
Facultat de Física, Universitat de Barcelona, Diagonal 645, 08028 Barcelona, Spain. and Barcelona Supercomputing Center (BSC), Barcelona, Spain.

Advisor: Alba Cervera Lierta
Barcelona Supercomputing Center (BSC), Barcelona, Spain.

Tutor: Juan José García-Ripoll
Institute of Fundamental Physics IFF-CSIC, Calle Serrano 113b, Madrid 28006, Spain.

The field of quantum computing has grown fast in recent years, both in theoretical developments and the practical construction of quantum computers. These computers were initially proposed, among other reasons, to efficiently simulate and comprehend the complexities of quantum physics. In this paper, we address this need by utilizing a scheme presented in previous works for the exact simulation of the 1-D XY model on a quantum computer. Using the Qibo framework, we successfully diagonalize the proposed Hamiltonian, enabling access to the complete energy spectrum. Furthermore, we propose a novel approach to design a quantum circuit to perform exact time evolution. Among all the possibilities the circuit could offer, we compute the ground and first excited state energies for the symmetric XY model with spin chains of $n = 4$ and $n = 8$ spins. Further, we calculate the expected value of transverse magnetization for the ground state in the transverse Ising model. Both studies allow the observation of a quantum phase transition from an antiferromagnetic to a paramagnetic state. Additionally, we have simulated the time evolution of the state all spins up in the transverse Ising model. The scalability and high performance of the algorithm make it an ideal candidate for benchmarking purposes, while also laying the foundation for simulating other integrable models on quantum computers.

I. INTRODUCTION

In the first decade of the XXI century, we witnessed an explosion of the quantum computing field driven by the incredible potential that quantum computing exhibits to solve some intractable classical problems [1]. Among these challenges, one of the enduring objectives of quantum computing is the simulation of quantum systems. Although several classical strategies exist for simulating such systems [2, 3], they often prove to be inefficient when dealing with complex quantum systems. Consequently, the simulation of these systems demands alternative methods for efficient execution. Quantum computers emerge as a promising solution to supply this demand. Due to their quantum essence, the simulation of strongly correlated systems is the natural arena where quantum computers are expected to show a clear advantage over classical ones, as Feynman stated in [4].

Despite having undergone considerable development during the last decade, quantum computing is still in an early stage. The current state of quantum computing is known as the Noisy Intermediate-Scale Quantum (NISQ) era [5], which has been characterized by constrained-size quantum processors (containing 50-100 qubits) with imperfect control over them (i.e. they are sensitive to their environment and prone to quantum decoherence and other sources of errors). In this context, it has become essential to have methods that allow companies and researchers to test the efficiency of their new devices or compare them. However, due to the limited number of qubits and the high error rate, finding proper algorithms for NISQ devices has become a difficult task. These algorithms need to be easy to escalate with the number of qubits and present a feasible circuit depth to avoid the large accumulation of noise.

This paper presents a circuit specifically designed for the NISQ era, offering the capability to explore intriguing phenomena such as quantum phase transitions. Our work consists in implementing a quantum circuit that performs the exact simulation of a one-dimensional (1-D) spin chain with an XY -type interaction. We programmed a set of Python libraries that allows the implementation of the circuit for systems with a power of 2 number of qubits using Qibo [6], an open-source framework for quantum computing. Qibo is the native language of the Barcelona Supercomputing Center quantum computer, which will allow the users to directly test this algorithm with real machines. The foundation of our work is based on Ref.[7, 8], where the steps followed to design the quantum circuit rest upon tracing and implementing the well-known transformations that solve the model analytically [9]. As a result, this technique can access the whole energy spectrum, enabling us to simulate any excited or thermal state and its dynamical evolution. In addition, this framework can be easily extended to other integrable models, including the Kitaev-honeycomb model [10], or to systems whose effective low-energy behavior can be suitably described by quasi-particles.

This paper is organized as follows: In Sec.II we describe the characteristics of the XY model and solve it analytically. Moving to Sec.III, we revisit the method introduced in Ref.[8] to construct an efficient circuit that

diagonalizes the XY Hamiltonian. Then, we present the circuit employed for simulating spin chains of $n = 4$ and $n = 8$ qubits. In Sec.V, we design a quantum circuit tailored for exact time evolution. Our simulations, utilizing the proposed quantum circuit, are detailed in Section VI. Finally, the conclusions are exposed in Sec.VII.

II. THE 1-D XY MODEL

The XY model is derived from the Heisenberg model [11] by introducing an easy-plane anisotropy. Those models are vastly used to study critical points and phase transitions of magnetic systems within the condensed matter field. Moreover, the XY model stands out for exhibiting a quantum phase transition between an antiferromagnetic state to a paramagnetic state. The $1-D$ XY Hamiltonian, considering the specific bound condition used for this system, can be written as

$$\begin{aligned}\mathcal{H}_{XY} = J\left(\sum_{i=1}^{n-1}\frac{1+\gamma}{2}\sigma_i^x\sigma_{i+1}^x + \frac{1-\gamma}{2}\sigma_i^y\sigma_{i+1}^y\right)\\ + \lambda\sum_{i=1}^{n}\sigma_i^z + J\frac{1+\gamma}{2}\sigma_1^y\sigma_2^z\cdots\sigma_{n-1}^z\sigma_n^y +\\ + J\frac{1-\gamma}{2}\sigma_1^x\sigma_2^z\cdots\sigma_{n-1}^z\sigma_n^x,\end{aligned} \tag{1}$$

where n is the number of spins in the 1-D spin chain, σ_j^i with $i = x, y, z$ is the Pauli matrix acting on the site j, J determines the behavior of the ordered phase (ferromagnetic for $J < 0$ and antiferromagnetic $J > 0$) γ is the anisotropic parameter and λ represents the strength of the transverse magnetic field.

The first two terms correspond to the $1-D$ XY Hamiltonian, whereas the last two terms appear due to boundary conditions. These boundary terms can be substituted with the conventional periodic terms $\sigma_n^x\sigma_1^x$ and $\sigma_n^y\sigma_1^y$ for states with an even number of spins pointing up, and the same terms with a negative sign for states with an odd number of spins pointing up. They arise as a consequence of imposing periodic boundary conditions on the fermionic modes and, subsequently, mapping them into spin operators. In the thermodynamic limit, the boundary conditions do not play any role and our Hamiltonian recovers the same results as in the 1-D XY case. For a deeper knowledge of boundary conditions and their effects in the XY model, see Ref.[12].

A. Jordan-Wigner transformation

Generally, quantum spin objects are notoriously difficult to deal with in many-body physics because they neither fulfill fermionic nor bosonic algebra. For this reason, the first step to diagonalize XY Hamiltonian consists in applying the Jordan-Wigner transformation [13], which maps the spin operators σ into spinless fermionic modes c:

$$\sigma_i^+ = c_i^\dagger\left(\prod_{l=1}^{i-1}-\sigma_l^z\right),\ \ \sigma_i^- = \left(\prod_{l=1}^{i-1}-\sigma_l^z\right)c_i, \tag{2}$$

where $\sigma^{+(-)}$ are the spin ladder operators. The new operators $c_i^\dagger$ and c_i are the spinless fermionic creation and annihilation operators, respectively. Hence, both operators follow the anticommutation rules $\{c_i, c_j^\dagger\} = \delta_{ij}$ and $\{c_i, c_j\} = \{c_i^\dagger, c_j^\dagger\} = 0$. After applying the Jordan-Wigner transformation, the Hamiltonian becomes

$$\begin{aligned}\mathcal{H}_c = \ J\ \sum_{i=1}^{n} c_i^\dagger c_{i+1} + c_{i+1}^\dagger c_i + \gamma\left(c_i^\dagger c_{i+1}^\dagger + c_{i+1}c_i\right) +\\ +\ \lambda\sum_{i=1}^{n}(2c_i^\dagger c_i - 1).\end{aligned} \tag{3}$$

B. Fourier Transform

The next step to diagonalize the Hamiltonian is applying the Fourier transform to pass from position to momentum space. In the second quantization, the Fourier transform is defined as:

$$c_j = \frac{1}{\sqrt{N}}\sum_{k=-\frac{n}{2}+1}^{\frac{n}{2}} b_k e^{i\frac{2\pi kj}{n}},\ \ c_j^\dagger = \frac{1}{\sqrt{N}}\sum_{k=\frac{-n}{2}+1}^{\frac{n}{2}} b_k^\dagger e^{-i\frac{2\pi kj}{n}}, \tag{4}$$

where $b_k^\dagger$ and b_k are the creation and annihilation operators of the fermionic Fourier modes. The discrete k values are determined establishing the translational invariance of the system. Once this transformation is applied, the Hamiltonian reads

$$\begin{aligned}\mathcal{H}_{FT} \ = \ \sum_{k=\frac{-n}{2}+1}^{\frac{n}{2}} 2\left(\lambda + J\cos\left(\frac{2\pi k}{n}\right)\right)b_k^\dagger b_k\\ +\ iJ\gamma\sin\left(\frac{2\pi k}{n}\right)\left(b_k^\dagger b_{-k}^\dagger + b_k b_{-k}\right) - \lambda n.\end{aligned} \tag{5}$$

It is noteworthy, at this point, that we have gone from an initial Hamiltonian, in which each fermion engages with the others by first neighborhood interaction, to one where only fermions with opposite momentum k interact between them.

C. Bogoliubov transformation

The final step to achieve a full disentanglement of the XY Hamiltonian corresponds to finding a transformation

that mixes k and $-k$ modes. This is implemented by the Bogoliubov transformations

$$\begin{aligned} a_k &= u_k b_k + v_k b_{-k}^\dagger, \qquad a_{-k} = u_{-k} b_{-k} + v_{-k} b_k^\dagger, \\ a_k^\dagger &= u_k^* b_k^\dagger + v_k^* b_{-k}, \qquad a_{-k}^\dagger = u_{-k}^* b_{-k}^\dagger + v_{-k}^* b_k. \end{aligned} \tag{6}$$

The coefficients $u_{k(-k)}$ and $v_{k(-k)}$ are attained by enforcing fermionic anticommutation relationships in the new operators and imposing the vanishing of non-diagonal terms in Eq.(5). Further development of intermediate steps can be found in Ref.[10]. Accordingly, the new fermionic operators a_k and $a_k^\dagger$ are

$$\begin{aligned} a_k &= \cos\left(\frac{\theta_k}{2}\right) b_k + i \sin\left(\frac{\theta_k}{2}\right) b_{-k}^\dagger, \\ a_k^\dagger &= \cos\left(\frac{\theta_k}{2}\right) b_k^\dagger - i \sin\left(\frac{\theta_k}{2}\right) b_{-k}. \end{aligned} \tag{7}$$

The angle θ_k corresponds to $\tan(\theta_k) = \frac{J\gamma \sin\left(\frac{2\pi k}{n}\right)}{\lambda + J\cos\left(\frac{2\pi k}{n}\right)}$.

Finally, the diagonal Hamiltonian has the form

$$\tilde{\mathcal{H}} = \sum_{k=\frac{-n}{2}+1}^{\frac{n}{2}} \left[2E_k \left(a_k^\dagger a_k - \frac{1}{2} \right) + \epsilon_k - \lambda \right], \tag{8}$$

where

$$\begin{aligned} \epsilon_k &= \lambda + J\cos(\frac{2\pi k}{n}), \\ E_k &= \sqrt{\left(\lambda + J\cos\left(\frac{2\pi k}{n}\right)\right)^2 + \left(J\gamma \sin\left(\frac{2\pi k}{n}\right)\right)^2}. \end{aligned} \tag{9}$$

Here, E_k are the energies related to having one fermion in the Bogoulibov mode k or $-k$.

III. QUANTUM CIRCUIT TO DIAGONALIZE THE XY MODEL

In this section, we procure a circuit $\mathcal{U}_{dis}$ that transforms a given Hamiltonian $\mathcal{H}$ into a non-interacting one $\bar{\mathcal{H}}$. Then, we can easily obtain all the eigenstates and a superposition of them in the spin basis by preparing a computational product state and applying $\mathcal{U}_{dis}^\dagger$. Even though constructing these disentangling circuits $\mathcal{U}_{dis}$ is challenging, we can try to map each step into a quantum gate for models that present analytical solutions.

For the case it concerns us, the XY Hamiltonian needs three gates: *i*) Jordan-Wigner transformation gate, *ii*) Fourier transform gate, *iii*) Bogoliubov transformation gate. In the end, the disentangling circuit will exhibit the structure

$$\mathcal{U}_{dis} = \mathcal{U}_{Bog}.\mathcal{U}_{FT}\mathcal{U}_{JW}. \tag{10}$$

It is key to bear in mind that there is a gap between the gates that can be applied theoretically in a quantum computer and the gates that we currently know how to implement in real devices. Therefore, all gates must be decomposed into basic gates that can be implemented experimentally by quantum computers. For some cases, there are analytical schemes to decompose in basic gates [14].

A. Jordan-Wigner circuit

The Jordan-Wigner transformation maps the spin states to a fermionic spinless mode. In terms of the wave function,

$$\begin{aligned} |\Psi\rangle &= \sum_{i_1,\ldots,i_n=0,1} \Psi_{i_1,\ldots,i_n} |i_1,\ldots,i_n\rangle = \\ &= \sum_{i_1,\ldots,i_n=0,1} \Psi_{i_1,\ldots,i_n} \left(c_1^\dagger\right)^{i_1} \cdots \left(c_n^\dagger\right)^{i_n} |0\rangle \,, \end{aligned} \tag{11}$$

where i_j represent the state i of the qubit at position j, with j going from 1 to the number of qubits n. In spin and fermionic space, the i can take values 0 or 1. In spin space, $|0\rangle = |+\rangle$ and $|1\rangle = |-\rangle$, while in fermionic space $|1\rangle_j$ $\left(|0\rangle_j\right)$ means the j-th position is (not) occupied by a fermion.

The relevant point is that the coefficients $\Psi_{i_1,\ldots,i_n}$ do not change after the transformation. Therefore, theoretically, no gate is necessary to perform the Jordan-Wigner transformation. However, two subtleties are worth commenting on.

The first one becomes relevant when two-qubit states are exchanged through a SWAP operation. Since we are working with fermions, introducing a minus sign is necessary when two states are, such as the state $|11\rangle$. This adjustment is achieved through the fermionic SWAP operation (fSWAP).

The second issue corresponds to a notational problem. In conventional terms, spin states are denoted $|+\rangle = |0\rangle$, while in n-body systems the vacuum state is written as $|0\rangle$, or sometimes, $|\Omega\rangle$. As Jordan-Wigner maps $|-\rangle$ into $|\Omega\rangle$, it has been decided to introduce an X gate to preserve vector notation and mitigate confusion. Consequently, the initial circuit ensemble will consist of a layer of X gates applied to each qubit.

B. Fourier transform circuit

The next step is to get the fermionic modes to momentum space by applying the Fourier transform (FT). For cases where the number of particles is $n = 2^m$, the fermionic Fourier transform can be implemented by following the scheme of the classical Fast Fourier Transform [15]. The idea is to decompose the n-qubit FT in two parallel $\frac{n}{2}$-qubit FT, one acting upon odd and even modes

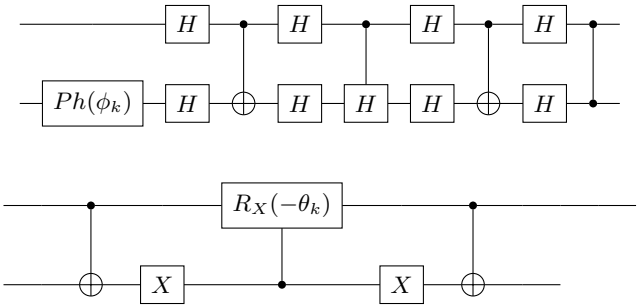

FIG. 1: The upper diagram shows the decomposition of the building block of F_k^n shown in Eq.(13), where $\phi_k = \frac{-i2\pi k}{n}$. The lower diagram shows the decomposition of the building block of B_k^n shown in Eq.(14), where θ_k is defined below Eq.(7).

respectively:

$$\sum_{j=0}^{n-1} e^{i\frac{2\pi}{n}jk} c_j = \sum_{j'=0}^{n/2-1} e^{i\frac{2\pi}{n/2}j'k} c_{2j'} + e^{i\frac{2\pi k}{n}} e^{i\frac{2\pi}{n/2}j'k} c_{2j'+1}. \tag{12}$$

This approach is detailed in Ref.[16]. In our case, the gate that implements such transformation is:

$$F_k^n \equiv \begin{pmatrix} 1 & 0 & 0 & 0 \\ 0 & \frac{-e^{-i\frac{2\pi}{n}k}}{2} & \frac{1}{\sqrt{2}} & 0 \\ 0 & \frac{e^{-i\frac{2\pi}{n}k}}{\sqrt{2}} & \frac{1}{\sqrt{2}} & 0 \\ 0 & 0 & 0 & -e^{-i\frac{2\pi}{n}k} \end{pmatrix}, \tag{13}$$

where k is the momentum mode. The basic gate decomposition of F_k^n is shown in Fig.1.

C. Bogoliubov transformation circuit

The Bogoliubov transformation described in Eq.(7) mixes creation and annihilation operators from k and $-k$ Fourier modes. Consequently, the vacuum changes after being implemented the Bogoliubov transformation. The new vacuum can be found in terms of the Fourier basis imposing $a_k |\Omega'\rangle = a_{-k} |\Omega'\rangle = 0$. Once the new vacuum is obtained, the remaining vectors can be derived by applying the creation operators $a_k^\dagger$ and $a_{-k}^\dagger$. The outcome of this process is a two-qubit gate, which is of the form

$$B_k^n \equiv \begin{pmatrix} \cos\left(\frac{\theta_k}{2}\right) & 0 & 0 & i\sin\left(\frac{\theta_k}{2}\right) \\ 0 & 1 & 0 & 0 \\ 0 & 0 & 1 & 0 \\ i\sin\left(\frac{\theta_k}{2}\right) & 0 & 0 & \cos\left(\frac{\theta_k}{2}\right) \end{pmatrix}, \tag{14}$$

with θ_k is described below Eq.(7). The basic gate decomposition of B_k^n is shown in Fig.1.

IV. SIMULATION FOR $n = 4$ AND $n = 8$ SPIN CHAIN

The explicit circuit $\mathcal{U}_{dis}$ for spin chains with $n = 4$ and $n = 8$ is illustrated in Fig.2, Fig.3, and Fig.4. As an example of the many applications facilitated by $\mathcal{U}_{dis}$, we have performed simulations to evaluate the ground state and first excited state energies for different values of λ in the symmetric XY model ($J = 1$ and $\gamma = 0$) for spin chains of $n = 4$ and $n = 8$. Computing the energy of the ground and the first excited state enables us to observe the quantum phase transition from an antiferromagnetic to a paramagnetic state.

For the case $n = 4$, the ground and the first excited state written in the diagonal basis are

$$|g\rangle = \begin{cases} |0100\rangle \\ |0000\rangle \end{cases} \quad |e\rangle = \begin{cases} |0000\rangle & \lambda \leq 1, \\ |0100\rangle & \lambda > 1. \end{cases} \tag{15}$$

For the case $n = 8$, the ground and the first excited state are

$$|gs\rangle = \begin{cases} |010\cdots0\rangle \\ |000\cdots0\rangle \end{cases} \quad |e\rangle = \begin{cases} |000\cdots0\rangle, & \lambda \leq 1, \\ |010\cdots0\rangle, & \lambda > 1. \end{cases} \tag{16}$$

Additionally, we have simulated the ground state for different values of λ in the transverse field Ising model ($J = 1$ and $\gamma = 1$) for the $n = 4$ spin chain. As it is one of the few physical observables that allows us to observe the phase transition between antiferromagnetic to paramagnetic ground state, the corresponding transverse magnetization has been computed. Analytically, taking into account that $\langle M_z \rangle = \sum_{i=1}^n \langle \sigma_i^z \rangle$ we get that

$$\langle gs|M_z|gs\rangle = \begin{cases} -\frac{\lambda}{2\sqrt{1+\lambda^2}}, & \lambda \leq 1, \\ -\frac{1}{2} - \frac{\lambda}{2\sqrt{1+\lambda^2}}, & \lambda \geq 1. \end{cases} \tag{17}$$

V. TIME EVOLUTION

The disentangling circuit $\mathcal{U}_{dis}$ designed for the 1-D XY model allows us to investigate the entire Hamiltonian spectrum with a simple application to the computational basis. This facilitates the computation of various system properties, including the expectation values of energy and magnetization. Nevertheless, there are situations where one is interested in studying dynamic properties. In such cases, we need to calculate the time evolution of the state, which can be a challenging task. However, a quantum circuit can be constructed to achieve exact time evolution for fermionic Hamiltonians that can be decomposed as the sum of the energies of each particle independently,i.e.

$$\mathcal{H} = \sum_{\alpha=1}^{N} \epsilon_\alpha a_\alpha^\dagger a_\alpha, \tag{18}$$

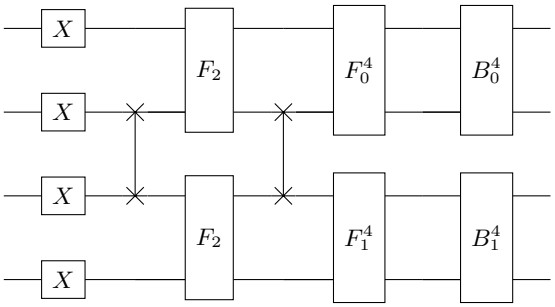

FIG. 2: Quantum circuit $\mathcal{U}_{dis}$ designed to diagonalize the XY Hamiltonian for $n = 4$ qubits. The initial layer consists of X gates, executing the Jordan-Wigner transformation. Subsequently, F_2 and F_k^n implement the fermionic Fourier Transform. The circuit concludes with the Bogoliubov transformation achieved by B_k^n. The SWAPs represented in the diagram correspond to fermionic SWAPs.

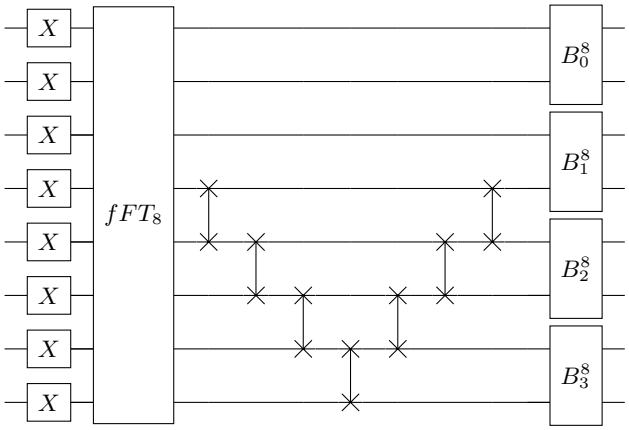

FIG. 3: Quantum circuit $\mathcal{U}_{dis}$ designed to diagonalize the XY Hamiltonian for $n = 8$ qubits. The initial layer consists of X gates, executing the Jordan-Wigner transformation. Subsequently, the fermionic Fourier Transform is applied by the circuit fFT_8, described in Fig.4. The circuit concludes with the Bogoliubov transformation achieved by B_k^n. The SWAPs represented in the diagram correspond to fermionic SWAPs.

where ϵ_α is the energy associated with having a particle in the state α, and $a_\alpha^\dagger$ (a_α) is the fermionic creation (annihilation) operator of the particle in the given state. For these Hamiltonians, the general time evolution operator $\mathcal{U}(t)$ can be decomposed into a tensor product of the time evolution operator for each qubit. To illustrate this, let us express the general time evolution of a state $|\psi(t)\rangle$ driven by a non-time-dependent Hamiltonian $\mathcal{H}$.

The time evolution in natural units is given by the unitary time-evolution operator

$$\begin{aligned} \mathcal{U}(t) &\equiv e^{-it\mathcal{H}}, \\ |\psi(t)\rangle &= \sum_l e^{-itE_l} |E_l\rangle \langle E_l| |\psi_0\rangle , \end{aligned} \tag{19}$$

where $|\psi_0\rangle$ is the initial state, $|E_l\rangle$ are the eigenstates of the given Hamiltonian, and E_l are the corresponding energies or eigenvalues of each state $|E_l\rangle$.

Due to the decomposable form of Hamiltonian in Eq.(18), eigenstates can be expressed as a product state of N states, each representing the presence or absence of a fermion in the α_i state:

$$|E_L\rangle = |\alpha_1\rangle \cdots |\alpha_N\rangle , \tag{20}$$

where $|\alpha_i\rangle$ can be represented by the qubits $|0\rangle$ or $|1\rangle$. Consequently, the action of the time evolution operator becomes

$$e^{-itE_l} |\alpha_1\rangle \cdots |\alpha_N\rangle = e^{-it\sum_{\alpha_1}^{N} \epsilon_\alpha a_\alpha^\dagger a_\alpha} |\alpha_1\rangle \cdots |\alpha_N\rangle . \tag{21}$$

Hence, the time evolution can be reinterpreted as

$$\mathcal{U}_1 |\alpha_1\rangle \cdots \mathcal{U}_n |\alpha_N\rangle , \tag{22}$$

where $\mathcal{U}_i$ is the time evolution operator for the i_{th} qubit.

A. Time evolution circuit for the XY model

The procedure described above tells us that, to construct the time evolution circuit, we just need to perform the time evolution for each qubit independently. Specifically, for the XY 1-D model, the time evolution for the qubit representing a fermionic particle with momentum k is

$$\mathcal{U}_k = e^{-it2E_k a_k^\dagger a_k} e^{-it[-E_k+\epsilon_k-\lambda]} = U_1 U_2. \tag{23}$$

The unitary operators U_1 and U_2 can be written in matrix form as

$$\begin{aligned} U_1 &\equiv \begin{pmatrix} 1 & 0 \\ 0 & e^{i\varphi_k} \end{pmatrix}, \\ U_2 &\equiv \begin{pmatrix} e^{i2\Phi_k} & 0 \\ 0 & e^{i2\Phi_k} \end{pmatrix}, \end{aligned} \tag{24}$$

where $\varphi_k \equiv -2tE_k$, and $\Phi_k \equiv -2t\,[-E_k + \epsilon_k - \lambda]$. The gate decomposition of $\mathcal{U}_k$ is shown in Fig.5.

As an example of the many possibilities this gate opens, let us compute the time evolution transverse magnetization expected value for the $n = 4$ qubits case, with $J = 1$, $\gamma = 1$, and $\lambda = 0.5$. Specifically, our initial state has all the spins aligned in the positive z direction, $|\psi(t = 0)\rangle = |\uparrow\uparrow\uparrow\uparrow\rangle$, which in the computational basis can be written as $|0000\rangle$. The first step to compute the time evolution consists in expressing the initial state in the eigenbasis of the XY Hamiltonian. This is achieved by applying the U_{dis} gate to the initial state, obtaining that

$$|\psi_0\rangle = \sin\left(\frac{\phi}{2}\right) |1100\rangle - i\cos\left(\frac{\phi}{2}\right) |1111\rangle , \tag{25}$$

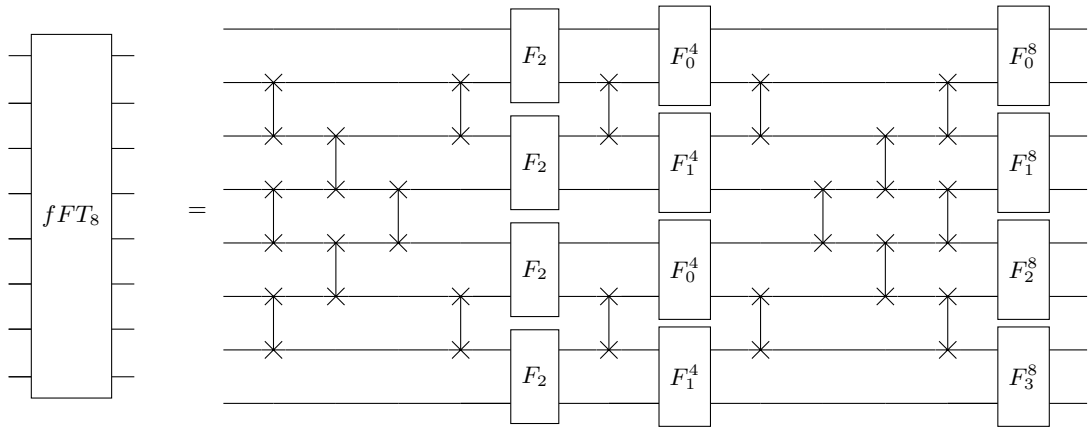

FIG. 4: Fermionic Fourier Transform circuit for the case $n = 8$. The SWAPs represented in the diagram correspond to fermionic SWAPs.

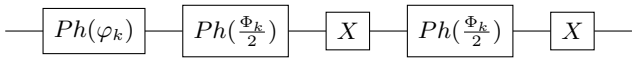

FIG. 5: In the diagram is shown the decomposition of the building block of $\mathcal{U}_k$ shown in Eq.(24), where $\varphi_k = -2tE_k$, and $\Phi_k = -2t\left[-E_k + \epsilon_k - \lambda\right]$.

where $\phi = \text{arctg}\left(\frac{1}{\lambda}\right)$. Subsequently, we apply the time evolution operator $\mathcal{U}(t)$ to obtain $|\psi(t)\rangle$. Then, the time-dependent state is

$$|\psi(t)\rangle = e^{+i4t\sqrt{1+\lambda^2}} \sin\left(\frac{\phi}{2}\right)|1100\rangle - i\cos\left(\frac{\phi}{2}\right)|1111\rangle\,, \tag{26}$$

where we have excluded the global phases from the result because they are not physically relevant. Lastly, we apply the circuit $U^\dagger$ to obtain the state in the spin representation. We can now compute analytically the expected value of the transverse magnetization, $\langle M_z\rangle$, which yields the result

$$\langle M_z\rangle = \frac{1 + 2\lambda^2 + \cos\left(4t\sqrt{1+\lambda^2}\right)}{2 + 2\lambda^2}. \tag{27}$$

VI. RESULTS AND DISCUSSION

In this section, we delve into the outcomes and insights derived from the application of our quantum circuit, $\mathcal{U}_{dis}$, across various scenarios. All the simulations for the spin chain $n = 4$ and $n = 8$ have been performed using the circuits represented in Figs. 2, 3, and 4.

Figure 6 presents the outcomes of the expected energy for the ground and first excited states in the symmetric XY model for spin chains with $n = 4$ and $n = 8$. Given the nature of quantum simulations, subject to inherent probabilistic uncertainties, each data point carries a statistical error proportional to $\frac{1}{\sqrt{N}}$, where N represents the number of shots, indicating the executions on a quantum processing unit (QPU). For our simulations, N was set to 1000. The results show the circuit's effectiveness in recovering analytical values for both cases. Moreover, a structural change in the ground state can be observed at $\lambda = 1$, where in the Bogoulibov basis the stablest state becomes the vacuum state ($|0\cdots0\rangle$ state) instead of having a fermion in the $-k$ mode ($|010\cdots0\rangle$ state) .

For the transverse field Ising model in the $n = 4$ spin chain, the results of the ground state's expected value of transverse magnetization $\langle M_z\rangle$ are shown in Fig. 7. The circuit successfully reproduces analytical values, and at $\lambda = 1$, a discontinuity appears due to a phase transition from an antiferromagnetic to a paramagnetic state.

We have also used the transverse field Ising model to explore the time evolution of the expected value of transverse magnetization $\langle M_z(t)\rangle$. The quantum circuit $\mathcal{U}(t)$ is employed to evolve the initial state $|\uparrow,\uparrow,\uparrow,\uparrow\rangle$ with the magnetic field strength fixed at $\lambda = 0.5$. Then, we use $\mathcal{U}_{dis}^\dagger$ to obtain the evolved spin state. The results are represented in Fig.8, showing satisfactory agreement between the quantum simulation and analytical values.

Despite the successful validation of the circuit, further analysis is required to assess its scalability and circuit depth as the number of qubits grows. As the Jordan-Wigner transformation is a simple layer of X gate, it escalates linearly with the number of qubits and the depth is constant. Similarly, the Bogoulibov transformation also presents a constant depth and the number of gates escalates proportionally to $\sim \frac{n}{2}$, where n represents the number of qubits. On the contrary, in Ref.[16], it is shown that the circuit depth of the Fourier transforms follows a logarithmic scaling of $\sim \log_2(n)$, with the number of gates increasing as $\sim n\log_2(n)$. Finally, the time evolution circuit scales linearly with the number of qubits n and presents a constant depth.

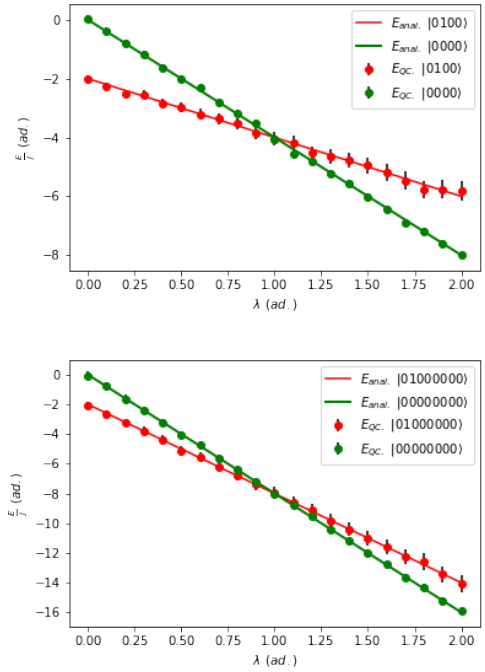

FIG. 6: Study of the ground and first excited state energy for the symmetric XY model as a function of the transverse field strength parameter λ. The upper image displays the results for a $n = 4$ spin chain, while the lower one illustrates the results for the case $n = 8$. The solid lines represent the analytical values of the energy E, while the scatter points correspond to the results obtained from a quantum computer simulation conducted in Qibo, utilizing the quantum circuit $\mathcal{U}_{dis}$.

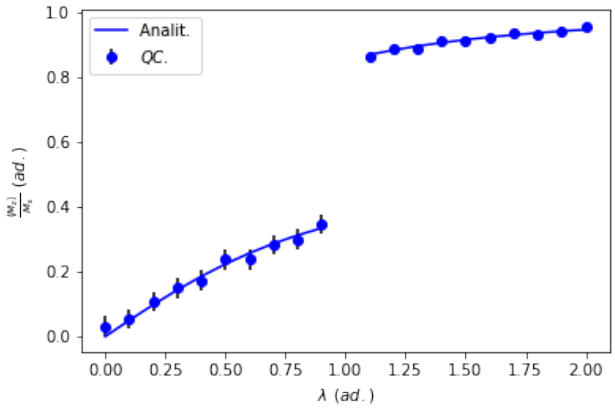

FIG. 7: The ground state's expected value of transverse magnetization $\langle M_z \rangle$ for the transverse field Ising model ($J = 1$ and $\gamma = 1$) in a spin chain with $n = 4$ as a function of the transverse field strength parameter λ. The solid line represents the analytical value of $\langle M_z \rangle$, while the scatter points correspond to the results obtained from a quantum computer simulation conducted in Qibo, utilizing the quantum circuit $\mathcal{U}_{dis}$.

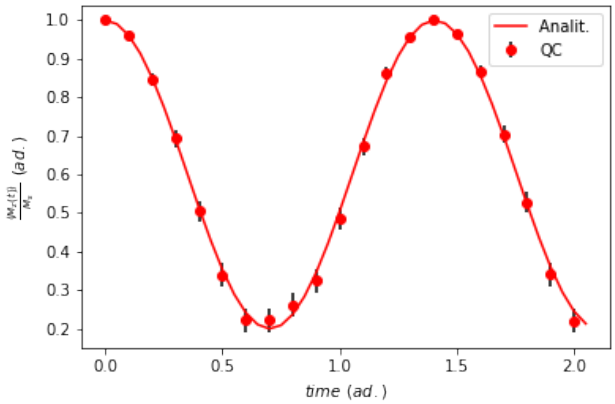

FIG. 8: Time evolution simulation of transverse magnetization $\langle M_z \rangle$ for the transverse field Ising model ($J = 1$ and $\gamma = 1$) in a spin chain with $n = 4$. The solid line represents the analytical value of $\langle M_z \rangle$, while the scatter points correspond to the results obtained from a quantum computer simulation conducted in Qibo, utilizing the quantum circuits $\mathcal{U}_{dis}$ and $\mathcal{U}(t)$.

VII. CONCLUSION

This paper presents a comprehensive implementation of the exact simulation of a 1-D XY spin chain on a digital quantum computer, simulated with the Qibo software. Our approach encompasses the entire steps of the analytical solution for this exactly solvable model, involving key transformations such as the Jordan-Wigner transformation, fermionic Fourier transform, and Bogoliubov transformation. We have also developed an algorithm to construct an efficient quantum circuit for powers of two qubits, capable of diagonalizing the XY Hamiltonian and executing its exact time evolution. Therefore, this circuit can be used to determine all the eigenstate vectors and it enables access to the complete energy spectrum, providing novel approaches for exploring various system properties, including energy, magnetization, and time evolution.

The quantum circuit developed in this paper serves as a benchmark for quantum computing devices. It presents efficient scalability with the number of qubits n, making it suitable to be used in devices of diverse sizes. Furthermore, the 1-D XY model's exact solvability not only allows us to test the efficiency of real quantum computers but also offers an avenue to study and model errors inherent in quantum computations, establishing a bridge between theoretical predictions and real-world outcomes.

Beyond its utility as a benchmark, the presented quantum circuit holds intriguing applications in condensed matter physics. The methods highlighted in this work can be extended to explore other integrable models, such as the Kitaev Honeycomb model [10], or with alternative ansatz, as seen in the Heisenberg model [11]. Additionally, there is potential to employ different strategies for

simulating thermal evolution [7] and it could open new paths to study quantum phase transition.

In conclusion, this paper contributes to the advancement of quantum computing algorithms and establishes a foundation for exploring quantum solutions to complex problems in condensed matter physics.

Acknowledgments

I am deeply grateful to Dr. Alba Cervera-Lierta for her generous time and guidance throughout this project. Her expertise and mentorship have provided me an invaluable experience. Also, I would like to thank the BSC Quantic group and Dr. Juan José García-Ripoll for the opportunity and help given.

[1] Fedorov, A.K., et al. (2018). Quantum computing at the quantum advantage threshold: a down-to-business review. *Quantum, 2*(79), 1-19. doi:10.22331/q-2018-08-06-79

[2] Blunt, N.S., et al. (2014). Density-matrix quantum Monte Carlo method. *Phys. Rev. B, 89*(24), 245124. doi:10.1103/PhysRevB.89.245124

[3] Orús, R. (2019). Tensor networks for complex quantum systems. *Nature Reviews Physics, 1*(9), 538-550. doi:10.1038/s42254-019-0086-7

[4] Feynman, R.P. (2018). Simulating physics with computers. In *Feynman and computation* (pp. 133-153). CRC Press.

[5] Preskill, J. (2018). Quantum Computing in the NISQ era and beyond. *Quantum, 2*(79), 1-8. doi:10.22331/q-2018-08-06-79

[6] Efthymiou, S., et al. (2021). Qibo: a framework for quantum simulation with hardware acceleration. *Quantum Science and Technology, 7*(1), 015018. doi:10.1088/2058-9565/ac39f5

[7] Cervera-Lierta, A. (2018). Exact Ising model simulation on a quantum computer. *Quantum, 2*(114), 1-19. doi:10.22331/q-2018-12-21-114

[8] Verstraete, F., Cirac, J.I., & Latorre, J.I. (2009). Quantum circuits for strongly correlated quantum systems. *Physical Review A, 79*(3), 032316. doi:10.1103/PhysRevA.79.032316

[9] Eriksson, E. (2008). Quantum Phase Transitions in an Integrable One-Dimensional Spin Model. (Doctoral dissertation, Chalmers University of Technology).

[10] Schmoll, P., & Orús, R. (2017). Kitaev honeycomb tensor networks: Exact unitary circuits and applications. *Physical Review B, 95*(4), 045112. doi:10.1103/PhysRevB.95.045112

[11] van der Sijs, A.J. (1993). Heisenberg models and a particular isotropic model. *Physical Review B, 48*(10), 7125-7133. doi:10.1103/PhysRevB.48.7125

[12] Yan He and Hao Guo. *The boundary effects of transverse field Ising model. Journal of Statistical Mechanics: Theory and Experiment*, **2017**(9), 093101 (2017). ISSN: 1742-5468. DOI: 10.1088/1742-5468/aa85b0.

[13] Jordan, P., & Wigner, E. (1928). Über das Paulische Äquivalenzverbot. *Z. Physik*. doi:10.1007/BF01331938

[14] Barenco, A., et al. (1995). Elementary gates for quantum computation. *Physical Review A, 52*(5), 3457-3467. doi:10.1103/PhysRevA.52.3457

[15] Brigham, E.O., & Morrow, R.E. (1967). The fast Fourier transform. *IEEE Spectrum, 4*(12), 63-70. doi:10.1109/MSPEC.1967.5217220

[16] Ferris, A.J. (2014). Fourier Transform for Fermionic Systems and the Spectral Tensor Network. *Physical Review Letters, 113*(1), 010401. doi:10.1103/PhysRevLett.113.010401